JACS
JOURNAL OF THE AMERICAN CHEMICAL SOCIETY
Article
pubs.acs.org/JACS

White Light Emission and Second Harmonic Generation from Secondary Group Participation (SGP) in a Coordination Network

Jun He,[†,§] Matthias Zeller,[‡] Allen D. Hunter,[‡] and Zhengtao Xu*[,†]

[†]Department of Biology and Chemistry, City University of Hong Kong, 83 Tat Chee Avenue, Kowloon, Hong Kong, China
[‡]Department of Chemistry, Youngstown State University, One University Plaza, Youngstown, Ohio 44555, United States

Supporting Information

ABSTRACT: We describe a white emitting coordination network solid that can be conveniently applied as a thin film onto a commercial UV-LED lamp for practical white lighting applications. The solid state material was discovered in an exercise of exploring molecular building blocks equipped with secondary groups for fine-tuning the structures and properties of coordination nets. Specifically, $CH_3SCH_2CH_2S$- and (*S*)-$CH_3(OH)CHCH_2S$- (2-hydroxylpropyl) were each attached as secondary groups to the 2,5- positions of 1,4-benzenedicarboxylic acid (bdc), and the resultant molecules (**L1** and **L2**, respectively) were crystallized with Pb(II) into the topologically similar 3D nets of Pb**L1** and Pb**L2**, both consisting of interlinked Pb-carboxyl chains. While the CH_3S- groups in Pb**L1** are not bonded to the Pb(II) centers, the hydroxy groups in Pb**L2** participate in coordinating to Pb(II) and thus modify the bonding features around the Pb(II), but only to a slight and subtle degree (e.g., Pb−O distances 2.941−3.116 Å). Interestingly, the subtle change in structure significantly impacts the properties, i.e., while the photoluminescence of Pb**L1** is yellowish green, Pb**L2** features bright white emission. Also, the homochiral side group in Pb**L2** imparts significant second harmonic generation, in spite of its seemingly weak association with the main framework (the NLO-phore). In a broad perspective, this work showcases the idea of secondary group participation (SGP) in the construction of coordination networks, an idea that parallels that of hemilabile ligands in organometallics and points to an effective strategy in developing advanced functions in solid state framework materials.

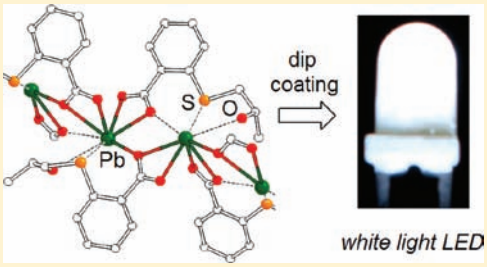

INTRODUCTION

The growing field of coordination networks[1] provides great opportunities for interfacing molecular chemistry with the development of functional framework materials. Thanks to the advances in the tectonic/building block approach for network design and construction, the metric scale and topological features of the framework can now be reasonably well correlated with the molecular size and geometry, with a large body of porous structures achieved as a result. The major forefront is now shifting toward functionalizing the host network by means of even closer interaction with molecular chemistry. A large, attractive exercise would be to implant in the organized framework matrix the structure and reactivity motifs established from the solution regime of molecular chemistry, in order for a close interplay to take root, and to generate new directions for the science of solid state materials. The use of secondary groups to modify molecular building blocks illustrates this megatrend of research.[2] By affixing secondary groups to a prototypal building block, one stands to couple the rich variety of organic functions to the prospective host network. A productive approach is to choose secondary groups that refrain from disruptive metal complexation that interferes with the primary groups in setting up the host coordination net. In other words, a clear "orthogonality" or "division of labor" between the primary and secondary groups is usually hoped for, i.e., the former bind to the metal centers and build up the net, while the latter remain nonbonded, and serve instead as free-standing functions decorating the host net.

In contrast to the above "orthogonal" approach, here we play on the idea of utilizing secondary group participation (SGP) in bonding to the metal centers, so as to fine-tune the coordination spheres of the metal centers and to impact the material properties. The goal is to explore secondary groups that bind to the metal centers, but in a rather weak and subtle fashion, so as to avoid disrupting the structural integrity of the scaffold set up by the primary links. In a cross-cutting light, the idea of SGP closely parallels that of hemilabile ligands in homogeneous metal-centered catalysis[3] − these are hybrid ligands containing two sets of donors: one binds strongly to the metal center, whereas the other does so weakly and reversibly. The latter may therefore pop off to allow the metal center to take up the substrate and hop back on to stabilize a reactive intermediate, thus facilitating the catalytic process. This imagery of a hemilabile donor coming on and off the metal center is suggestive of a potential solution to the topical issue of achieving accessible metal sites in coordination networks.[2f,4] Namely, SGP could serve to temporarily block a coordination site on the metal center (while the main framework is being

Received: August 5, 2011
Published: December 13, 2011

dx.doi.org/10.1021/ja2073559 | J. Am. Chem.Soc. 2012, 134, 1553−1559

assembled) and later on open up to accommodate the guest donors.

As a preliminary advance in utilizing SGP for functionalizing framework materials, we here illustrate how the subtle bonding effect from SGP could significantly impact the solid state properties. Reported below is a comparative study on two Pb^{II}-based nets from molecules H_2**L1** and H_2**L2** (Scheme 1): Pb**L1** and Pb**L2** (henceforth **1** and **2**, respectively). Although **1** and **2** feature similar network topologies (based on the Pb^{II}–carboxylate interactions), the side chains impart a subtle yet significant difference. In **1**, the methylthio unit on the side chain is not associated with the Pb^{II} ion; while in **2**, the hydroxy group of the homochiral side chain is in contact with Pb^{II} and generates, within a single, monolithic structure, the functional combination of white light photoluminescence and second harmonic generation (SHG).

Scheme 1

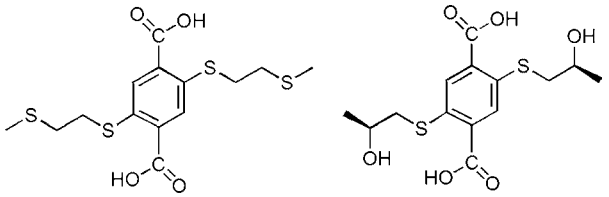

EXPERIMENTAL SECTION

The general procedures, as well as the synthetic procedures for **L1** and **L2** are included in the Supporting Information (SI).

Crystallization of 1. **L1** (3.8 mg, 10.0 μmol) and $Pb(NO_3)_2$ (5.2 mg, 15.7 μmol) were loaded into a heavy-wall glass tube (soda lime, 10mm OD, 6mm ID), and then a solution of water and acetonitrile (1 mL, 1:1, v/v) was added. The tube was then flame-sealed and heated at 100 °C in a programmable oven for 48 h, followed by slow cooling (0.1 °C/min) to room temperature, during which yellow prism single crystals suitable for single-crystal X-ray diffraction were formed (4.8 mg, 83% yield based on **L1**). Chemical analysis of the product $C_{14}H_{16}O_4PbS_4$ yielded the following: calcd [C (28.81%), H (2.76%)]; found [C (28.92%), H (2.61%)]. IR (ν/cm^{-1}): 3433 (w), 2970 (w), 2908 (m), 2819 (w), 1523 (s), 1429 (w), 1383 (s), 1320 (w), 1259 (m), 1203 (w), 1091 (w), 986 (w), 904 (w), 845 (s), 788 (s), 691 (w), 621 (m), 567 (w), 512 (w). X-ray powder diffraction of the bulk sample indicated a pure phase consistent with the single-crystal structure (Figure S1). Compound **1** is insoluble in common organic solvents or water.

Crystallization of 2. A mixture of **L2** (3.5 mg, 10.0 μmol), $Pb(NO_3)_2$ (5.0 mg, 15.1 μmol) and dimethylformamide (DMF)–H_2O (1 mL, 2:1, v/v) was sealed and heated at 85 °C in a programmable oven for 48 h, followed by slow cooling (0.1 °C/min) to room temperature. Colorless plate-like single crystals suitable for single-crystal X-ray diffraction were formed (4.7 mg, 85% yield based on **L2**). Chemical analysis of the product $C_{14}H_{16}O_6PbS_2$ yielded the following: calcd [C (30.48%), H (2.92%)]; found [C (30.33%), H (3.03%)]. IR (ν/cm^{-1}): 3378 (m), 2970 (m), 2960 (m), 2916 (m), 2858 (w), 1551 (s), 1460 (w), 1385 (s), 1265 (m), 1113 (m), 1093 (w), 1030 (w), 939 (w), 853 (m), 846 (m), 788 (w), 749 (w), 650 (m), 590 (w), 505 (w). X-ray powder diffraction of the bulk sample indicated a pure phase consistent with the single-crystal structure (Figure S2). Compound **2** is insoluble in common organic solvents or water.

RESULTS AND DISCUSSION

Syntheses and Structural Studies. Both molecules **L1** and **L2** can be conveniently prepared from 2,5-dimercapto-1,4-benzenedicarboxylic acid (H_4DMBD) (see also the SI).[5] Compound **1** (composition: Pb·**L1**) was formed by reacting **L1** with $Pb(NO_3)_2$ in acetonitrile and water (1:1, v/v) under solvothermal conditions. X-ray single crystals of **1** (in centrosymmetric space group $C2/c$, No. 15) feature chains of the Pb-carboxyl component integrated into a 3D network by the aromatic cores of the **L1** molecules (Figure 1). The asymmetric unit of the unit cell of **1** consists of one-half of a Pb^{2+} ion (situated at the special position 0, 1.02, 1/4) and one-half of the centrosymmetric **L1** molecule. Each Pb^{2+} ion is coordinated to six carboxyl O atoms (from four **L1** molecules; Pb–O distances: 2.486, 2.551, and 2.686 Å) and two S atoms at significantly longer distances of 3.159 and 3.403 Å. The coordination geometry is rather lopsided, with all O and S donors confined mostly in one hemisphere, indicating significant $6s^2$ lone pair effect, which can be rationalized by mixing the 6s orbital with the 6p states (on the metal) as well as the 2p states from the ligand O atoms.[6] Notice that only the S atom right next to the carboxyl group is in contact with the Pb(II) ion, the other one further down the side chain (that of the $-SCH_3$) is not bonded, and remains free-standing. Of the two crystallographically inequivalent O atoms, O1 is shared by two Pb ions at 2.551 and 2.686 Å (while O2 is bonded to one single Pb ion at 2.486 Å), and each pair of adjacent Pb ions are bridged by two symmetry-related O1 atoms (Pb–Pb distance: 4.294 Å, see also see Figure 1). The overall feature of rod-packing in **1** is therefore similar to the reported MOF-70 (PbBDC; BDC: 1,4-benzenedicarboxylate)[7] and PbTMBD [TMBD: tetrakis(methylthio)-1,4-benzenedicarboxylate].[4e]

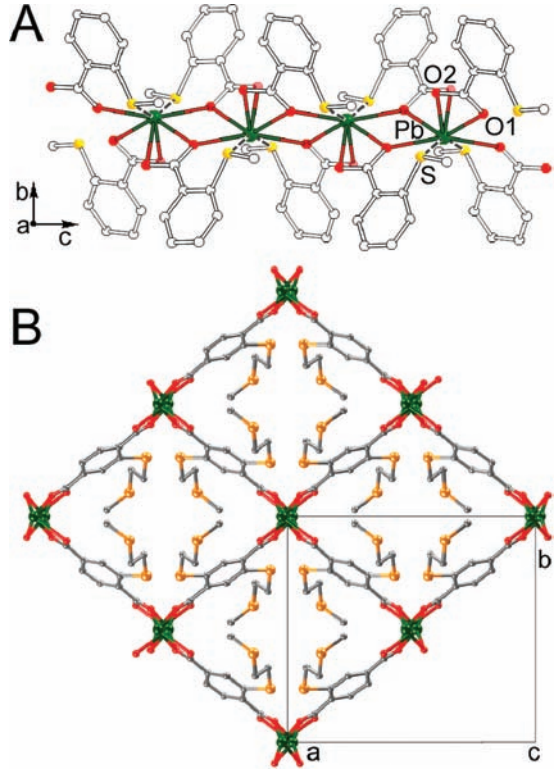

Figure 1. Crystal structure of **1**. (A) Local coordination environment around the Pb^{2+} ion (only the first S and C atoms are shown for the side chain. (B) View of the 3D coordination net along the c axis. H atoms and disordering of side chain atoms are omitted.

dx.doi.org/10.1021/ja2073559 | J. Am. Chem.Soc. 2012, 134, 1553–1559

Compound **2** was obtained from solvothermally reacting **L2** and $Pb(NO_3)_2$ in dimethylformamide and water (2:1, v/v) as colorless, plate-like crystals. This structure also builds on a similar rod-packing motif with the Pb-carboxylate rods linked by the aromatic moieties into a 3D net (Figure 2). However,

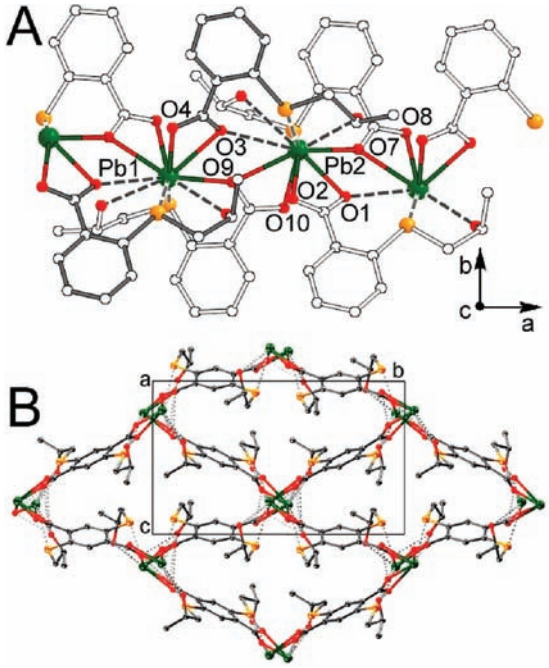

Figure 2. Coordination environment of the Pb^{2+} ions in **2** with atom labeling (a), and view of the 3D net of **2** along the *a* axis (b). H atoms are omitted.

the homochiral 2-hydroxypropyl side chain of **L2** imposes a chiral space group ($P2_1$; No. 4), with the asymmetric portion of the unit cell comprising two Pb^{2+} centers and two **L2** molecules (Figure 2a, see Figure S3 for more detailed atom labeling). The hydroxy side chains also impacts the local bonding environments of the Pb(II) ions. First, the S and O atoms from each side chain are bonded (chelated) to a common Pb ion [distances for the 4 side chains: (O6−Pb2, 2.941; S1−Pb2, 3.261 Å), (O12−Pb2, 3.116; S4−Pb2, 3.120 Å), (O5−Pb1, 3.010; S2−Pb1, 3.416 Å), (O11−Pb1, 2.984; S3−Pb1, 3.182 Å)], whereas one of the bridging carboxyl O−Pb bonds on each Pb ions is substantially elongated (O1−Pb1, 3.376; O3−Pb2, 3.347 Å; the other five O−Pb1 distances: 2.480, 2.579, 2.457, 2.636, 2.863; the other five O−Pb2: 2.497, 2.533, 2.482, 2.735, 2.583 Å). Notice also that the side chain and its *ortho*-carboxyl neighbor are bonded to two adjacent, separate Pb ions. In comparison with the O−Pb distances (2.486, 2.551, 2.686 Å) in **1**, the overall carboxyl-Pb interaction in **2** appears to be significantly weakened, and the adjacent Pb ions in **2** become farther apart at 4.785 Å (i.e., the −OH serves to push the carboxyl groups away from the Pb^{2+}). Because the photoluminescence process is closely related to the electronic interaction across the Pb^{2+} centers and the organic π−systems, the weakened carboxyl−Pb interaction in **2** might be related to the distinct white color of the photoluminescence of this material (as will be discussed again below).

The hydroxy (−OH) groups also form significant hydrogen bonds with the carboxylate O atoms O12−O3, 3.110; O11−O10, 2.889; O6−O4, 2.793; O5−O2, 2.697 Å. Even though the H-bonding might also modulate the photoluminescence processes (e.g., the vibrational relaxation and lifetime of the excitation states), its precise role remains unclear to us at this stage. The H-bonding to the carboxyl groups also further polarizes the O−H bonds and draws them near the Pb centers, which, we suspect, might have served to promote the coordination to the Pb^{2+} ions. By comparison, similar factors are absent in compound **1** to facilitate the bonding of CH_3S-groups to the Pb^{2+} ion. Moreover, the thioether S is a soft and relatively weak donor,[8] while the Pb^{2+} ion, as a borderline hard/soft acid (e.g., chemical hardness η_A values: Hg^{2+}, 7.7; Pb^{2+}, 8.5; Zn^{2+}, 10.8),[9] apparently does not make for stronger affinity for the thioether S atom, in other words, a softer species, like the Hg^{2+} ion, would have been more prone to bond with the thioether group.

Photoluminescence Properties. White light emitting materials and devices (e.g., light emitting diodes, LED)[10] are of great technological importance for next-generation solid state lighting and display applications. In this regard, single-component white light emitters offer advantages for fabrication and processing, as these circumvent the often complex procedures of mixing different phosphors to generate the color compositions for the desired "whiteness" (e.g., a blending of blue and yellow). Coordination/hybrid networks offer rich opportunities for developing single-component white light emitters,[11] mainly because the ligand-centered, charge transfer as well as metal-centered emission processes can potentially all be modulated in their relative intensities and wavelength positions, in order for the overall emission to attain the white light quality. In this vein, main group metals like lead and bismuth[11g,12] are of interest because (1) their ns^2np^0 configuration and the stereochemically active lone pairs often give rise to substantial photoluminescent processes involving the metal centers, contrasting, for example, the Zn^{2+}-based MOF-5 systems in which the photoluminescence has been found to be mostly ligand-based;[5c,13] (2) as heavy p-block elements, they tend to display flexible coordination behaviors, e.g., variable bonding distances, with secondary interactions furnishing a 7-fold (or higher) coordination configuration. Such flexible coordination is exemplified in the Pb−S and Pb−O secondary interactions in **1** and **2**, and provides an especially handy medium to engage the secondary groups (i.e., via SGP) in the structural and property modifications of the main framework.

Under UV radiation at RT, the solid sample of **2** exhibits a bright, white luminescence, whereas the emission from **1** appears yellowish green. For comparison, we first present the photoluminescence spectra of the corresponding free ligands of **L1** and **L2** in THF solutions. As shown in Figure 3, **L1** and **L2** display similar emission spectra with each consisting of a broad band that peaks around 450 nm (451 nm for **L1**, 456 for **L2**, with excitation wavelength λ_{ex} = 370 nm), and the emissions are blue in color. Such emissions observed of the free ligands in solutions can be assigned to the typical ligand-centered transitions (e.g., $\pi^* \rightarrow n$, $\pi^* \rightarrow \pi$).

The ligand-centered emission features are carried over into the room-temperature emission spectra of **1** and **2** (Figure 4), and they correspond to the high energy (HE) bands with emission maxima at 468 and 459 nm, respectively. Substantial differences, however, exist in the low energy (LE) bands of the emission spectra. Specifically, **1** features a dominant and broad emission band which peaks at 531 nm (the green region), resulting in an overall emission color of yellowish green for **1**.

dx.doi.org/10.1021/ja2073559 | *J. Am. Chem.Soc.* 2012, 134, 1553−1559

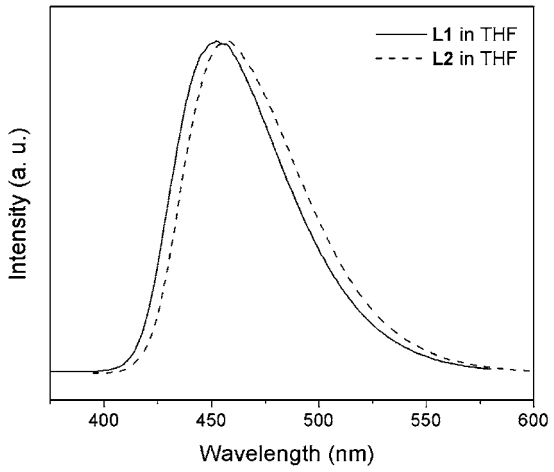

Figure 3. Room temperature emission spectra of **L1** and **L2** in THF (5×10^{-5} M, λ_{ex} = 370 nm).

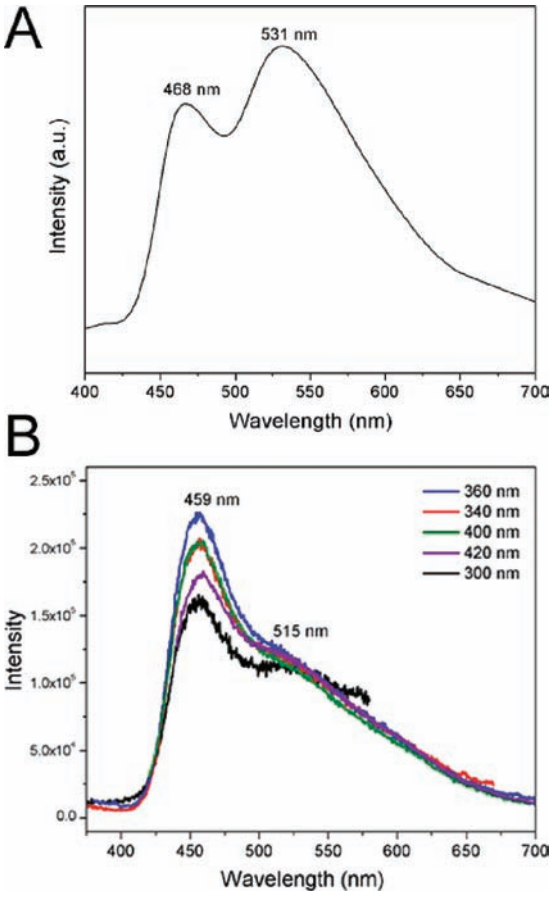

Figure 4. Room temperature emission spectra of (a) **1** in the solid state (λ_{ex} = 365 nm) and (b) **2** in the solid state under the excitation of 300, 340, 360, 400, and 420 nm.

By comparison, the LE emission band of **2** becomes weaker than its HE band, with a "fat" tail spreading well into the red region beyond 600 nm. The major upshot is a decrease of the green contribution in the emission spectra of **2**, leading to a distinct white emission.

As also shown in Figure 4, the emissions of **1** and **2** respond differently to the variation of excitation wavelengths. For excitation wavelengths between 320 and 420 nm, the emission features of **1** stay mostly unchanged. As for **2**, the intensity of the HE emission band increases with the excitation wavelengths changing from 300 to 360 nm, and decreases from 360 to 420 nm; but no apparent changes occur on the LE band. Nevertheless, the overall emissions of **2** remain well within the white domain of the chromaticity diagram throughout the excitation wavelength range from 300 to 400 nm (Figure 5). The remarkable persistence of the white light feature observed

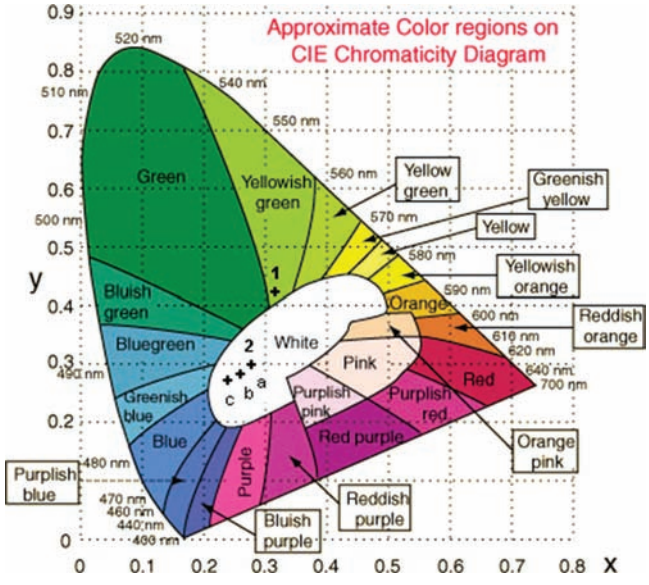

Figure 5. CIE-1931 chromaticity diagram and the positions (marked by the crosses) for emissions of **1** (λ_{ex} = 365 nm) and **2** [irradiated by 300 (a), 350 (b), and 400 nm (c)].

of **2** is rare, and provides advantages for lighting applications. Measurements on the powder sample of **2**, using the integration sphere setup,[14] indicates a fluorescence quantum efficiency on the order of 2−3%. Notice though that the integration sphere method tends to underestimate the actual value because of reabsorption of the emitted light by the sample;[14c,15] the underestimation could have been especially significant for **2**, which exhibits strong overlap between the emission and absorption, e.g., between 450 and 550 nm (see more in the SI, e.g., Figure S4). Nevertheless, the quantum efficiency found here is relatively low (even though the photoluminescence appears quite bright to the eye, e.g., see Figure 6), being comparable to a white emitting nanocrystal sample of CdSe.[16]

The colors of the emissions can be better quantified with the CIE (Commission Internationale de l'Eclairage) chromaticity

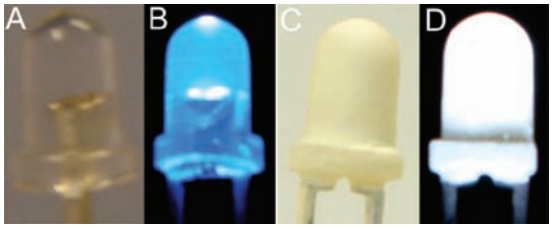

Figure 6. Photographs of LEDs: (A) a 3 mm reference UV LED (not turned on, available from Le Group Fox, Inc.); (B) the same UV LED turned on—the emission has a blue tinge; (C) the same LED coated with a thin layer of compound **2** (not turned on); (D) the coated LED turned on and illuminating bright white light.

dx.doi.org/10.1021/ja2073559 | J. Am. Chem.Soc. 2012, 134, 1553−1559

diagram, which serves to specify how the human eye perceives light with a given spectrum.[17] For this, the spectrum is deconvoluted into three functions related to the primary color components of red, green and blue. The (three) coefficients for the functions are then normalized (this leaves out the brightness factor) to give the two independent variables x and y. The coordinates (x, y) thus derived specify the chromaticity (color) of the spectrum. As seen in Figure 5, the chromaticity coordinates for **1** (spectrum of Figure 4a) are (0.31, 0.42), which is located in the yellowish green gamut. By comparison, the coordinates for the emissions of **2**, when excited by 300, 350, and 400 nm light are (0.27, 0.30; a), (0.25, 0.29; b), and (0.24 0.28; c), respectively, all falling within the white gamut of the CIE-1931 color space chromaticity diagram (Figure 5).

The LE bands centering around 531 and 515 nm in the emission spectra of **1** and **2** can be attributed to ligand-to-metal charge transfer (LMCT) between the aromatic π systems and the p orbitals of the Pb^{2+} centers, whereas the tailing features beyond 600 nm are suggestive of metal-centered transitions involving the s and p orbitals of s^2-metal cluster compounds.[12f−l] The white light emission in **2** therefore stems primarily from its LMCT being significantly reduced relative to the ligand-centered transitions; whereas for **1**, the LMCT appears to be more efficient and its emission band becomes stronger than that of the intraligand transitions. In this light, the weakened LMCT in **2** relates well to its weaker Pb^{2+}−carboxyl interactions that are caused by the perturbation of the −OH groups (see above discussion of the crystal structures). By comparison, in **1**, the Pb^{2+}−carboxyl interactions are stronger, which might have led to more effective electronic coupling between the aromatic π systems and the metal center. In other words, the intraligand excitation in **1** is therefore more effectively diverted and channeled to the metal center to generate the dominant LMCT feature.

Emission spectra taken at the lower temperature of 77 K are also informative (Figure S5). Specifically, the intraligand transition bands (around 450 nm) are largely diminished both for **1** and **2**, suggesting that the intraligand excitation is more effectively channeled to the metal center at low temperature (presumably because less thermal motion exists to perturb such channeling). While the residual intraligand emission of **1** at 77 K becomes hardly observable, that of **2** is more significant. The relative intensity of the intraligand bands observed here is in line with the rt data in Figure 4 and also points to more efficient LMCT in **1**. In addition, like at rt, **1** continues to show a LMCT band at the longer wavelength (peaking at 540 nm), compared with the 520 nm for **2**. The longer wavelengths of the LMCT in **1** (both at rt and 77 K) appear to be correlated with its stronger Pb-carboxyl interaction (as compared with the case of **2**), which is also consistent with an earlier observation that stronger Pb−O linkages in similar Pb-carboxylate systems are associated with larger red shifts of the related emission bands.[12e]

The photoluminescent processes in coordination networks are, however, complex, and the emission characteristics (e.g., position and intensity of the peak) can be greatly influenced by the structures and conformations (e.g., rigidity) of the molecules. The recently reported Bi(III) and Pb(II) pyridine-2,5-benzenedicarboxylate networks, for example, exhibit MLCT bands that, unlike the current systems, are instead blue-shifted relative to the ligand emissions.[11g] Further electronic structure calculations are needed for elucidating the structure−property correlations in these and related photoluminescent networks. Along this direction, using side chains as secondary functions offers unique opportunities for systematically modifying and fine-tuning the prototypal framework structure, and for probing, within the matrices of structurally well-defined crystalline frameworks, how structural changes impact photoluminescent properties.

Fabrication of White Light LED. By a simple and efficient dip coating procedure, a thin film of compound **2** can be applied onto a commercially available UV-LED lamp (similar to that of Ki and Li[11b]), and thus accomplish the conversion into a new LED that emits bright white light (Figure 6). Specifically, an as-made crystalline sample of **2** (about 10 mg) was loaded into an agate mortar and manually ground with the pestle for 20 min to afford a fine powder. Ethanol (1.0 mL, ABS) was then added to the mortar. Further grinding (for about 1 min) was applied until a significant portion of the alcohol has evaporated and a homogeneous slurry was achieved. A commercial 360 nm UV-LED lamp (Le Group Fox, Inc.) was then dipped into the slurry, held therein for several seconds, and then taken out for the coating to dry in air. This dip coating process can be repeated to further ensure an even and continuous coating of **2** on the lens/housing of the LED. The performance of the white light LED thus fabricated is stable for months in air and the white color quality remains consistent over a wide temperature range (e.g., −20 °C to rt). This simple experiment serves to demonstrate the use of compound **2** in a practical lighting application.

Quadratic Nonlinear Optical Properties. Progress in the crystal engineering of coordination networks provides helpful insight into the control of acentric assembly of polar and multipolar organic molecules, so as to impact the diverse properties of second harmonic generation, piezoelectrics, pyroelectrics and ferroelectrics.[18] Considerable efforts have been devoted to addressing the intriguing issue of assembling nonchiral molecules into acentric networks. For example, Ward and co-workers devised guanidinium sulfonate (GS) sheets to orient the pillar groups in polar order.[19] Another notable approach builds on the interplay of dipolar linkers and interpenetration, e.g., an odd-fold interpenetration of diamondoid nets is perforce acentric.[18c] Along this line, we have explored star-shaped molecules as building blocks that effectively preclude interpenetration, so as to preserve the acentricity of 3D nets.[20] Subsequent developments include the construction of octupolar networks[21] and the use of backfolded molecules to induce acentric features in solid state networks.[22]

A commonality of these ideas is to focus on the backbone of the molecule, and to design its shape and function so as to induce acentricity on the main grid of the framework. Quite often, one aims for frameworks featuring connectivities (topologies) that are inherently acentric (e.g., the diamondoid or gyroid net), and is thus limited to frameworks as such. By comparison, by attaching chiral side groups to the molecular backbone, one can hope to relay the chiral character to the main grid, and thus work to include networks of acentric topologies in their prototypal forms. However, a key question remains: could the acentric information from the side groups be effectively imparted to the main grid, so as to achieve, e.g., significant quadratic NLO properties? For this, close interactions with the main frame as effected by SGP is especially pertinent. The structure of **2**, with the homochiral 2-hydroxypropyl side chain in well-defined contacts with the Pb(II) centers of the main framework, provides an opportunity

to probe the impact of the side chain chirality upon the main framework.

The homochiral side chains impose the polar space group $P2_1$ on the crystal structure of **2**. However, the structure exhibits a pseudoinversion center (located at 0.242, 0.249, and 0.490) with an 81% fit for the space group $P2_1/c$ ($P2_1/a$ in the used setting). Specifically, the main grid and most of the side chain atoms fit the pseudoinversion symmetry; the only nonfitting atoms are the terminal O and C atoms on the side chain (i.e., O11, O12, C25, and C28). With the framework consisting of the more polarizable Pb-organic π structures as the major NLO chromophore, it would be remarkable if the very subtle structural influence from the side chains, so subtle as to keep the formal inversion symmetry of the main frame atoms, shall prove to be impactful on the NLO properties. Measurement of the second harmonic generation (SHG) by the Kurtz powder method[18a,23] found that compound **2** is nonphase-matchable and exhibits a significant SHG efficiency about 40 times larger than α-SiO_2 (for 45−63 μm particle size, see also Figure S6). Such preliminary results suggest effective impact from the chiral side chain, in spite of the pseudoinversion symmetry of the main framework. Because the solid of **2** also features significant emission intensity around 532 nm, a contribution from photoluminescence to SHG efficiencies can not, however, be completely ruled out at this stage. Further experimental studies based on the systematic and flexible modification of the secondary groups shall unveil more cases of SGP-induced acentric properties in coordination networks, in order to test the generality of this approach in preparing acentric materials, and to provide a basis for establishing the structure−property correlation thereof.

CONCLUSION AND OUTLOOK

The comparative studies on compounds **1** and **2** serve to highlight a potential merit of secondary group participation (SGP) for tailoring framework properties, as what appears to be delicate modulation on the structure could have significant effects on the solid state properties. Such an effect is well illustrated in the large impact on the distinct white light emission and NLO properties arising from the subtle interaction between the secondary −OH groups and the Pb^{2+} centers in **2**. In a larger perspective, we foresee SGP to be a potentially versatile approach to synergize organic chemistry and crystal engineering, in order to fully enlist the rich variety of organic/inorganic functions in advancing the science of framework materials. In parallel to the hemilabile ligands in catalytic metal complexes, one can imagine installing SGP motifs (like that of the Pb^{II}-hydroxy motif in **2**) within a porous framework to provide potentially active metal sites, i.e., the SGP initially serves to cap a coordination site, but ever so mildly so that it could be dislodged by a functional substrate in sensing, separation, catalysis, or other practical contexts.

ASSOCIATED CONTENT

Supporting Information

Additional experimental procedures, full crystallographic data in CIF format, X-ray powder diffraction patterns, low-temperature emission spectra and diffusion reflectance spectra for **1** and **2**, quantum yield measurement procedures, second harmonic generation (SHG) curve, and TGA plot of **2**. This material is available free of charge via the Internet at http://pubs.acs.org.

AUTHOR INFORMATION

Corresponding Author

*zhengtao@cityu.edu.hk

Present Address

[§]Faculty of Chemical Engineering and Light Industry, Guangdong University of Technology, Guangzhou 510006, Guangdong, China.

ACKNOWLEDGMENTS

We thank Drs. P. Shiv Halasyamani and Jeongho Yeon at the University of Houston for conducting the SHG measurement and analysis for compound **2**. This work is supported by the Research Grants Council of the Hong Kong Special Administrative Region [Project 9041437 (CityU 103009) and Project CUHK2/CRF/08] and City University of Hong Kong (Project No. 7002590). The single crystal diffractometer was funded by NSF Grant 0087210, by the Ohio Board of Regents Grant CAP-491, and by YSU. We thank Mr. Chen Yang and Mr. Kai Li from Prof. Chi-Ming Che's group at HKU for assistance with the quantum yield measurement and Dr. Zhengqing Guo for photographing the LEDs.

REFERENCES

(1) (a) Thomas, K. M. *Dalton Trans.* **2009**, 1487. (b) Férey, G. *Chem. Soc. Rev.* **2008**, *37*, 191. (c) Robson, R. *Dalton Trans.* **2008**, 5113. (d) Kitagawa, S.; Matsuda, R. *Coord. Chem. Rev.* **2007**, *251*, 2490. (e) Bradshaw, D.; Claridge, J. B.; Cussen, E. J.; Prior, T. J.; Rosseinsky, M. J. *Acc. Chem. Res.* **2005**, *38*, 273. (f) Lee, S.; Mallik, A. B.; Xu, Z.; Lobkovsky, E. B.; Tran, L. *Acc. Chem. Res.* **2005**, *38*, 251. (g) Ockwig, N. W.; Delgado-Friedrichs, O.; O'Keeffe, M.; Yaghi, O. M. *Acc. Chem. Res.* **2005**, *38*, 176. (h) Suslick, K. S.; Bhyrappa, P.; Chou, J. H.; Kosal, M. E.; Nakagaki, S.; Smithenry, D. W.; Wilson, S. R. *Acc. Chem. Res.* **2005**, *38*, 283.

(2) (a) Kiang, Y.-H.; Gardner, G. B.; Lee, S.; Xu, Z.; Lobkovsky, E. B. *J. Am. Chem. Soc.* **1999**, *121*, 8204. (b) Kiang, Y.-H.; Gardner, G. B.; Lee, S.; Xu, Z. *J. Am. Chem. Soc.* **2000**, *122*, 6871. (c) Xu, Z.; Lee, S.; Kiang, Y.-H.; Mallik, A. B.; Tsomaia, N.; Mueller, K. T. *Adv. Mater.* **2001**, *13*, 637. (d) Xu, Z.; Kiang, Y.-H.; Lee, S.; Lobkovsky, E. B.; Emmott, N. *J. Am. Chem. Soc.* **2000**, *122*, 8376. (e) Brunet, P.; Demers, E.; Maris, T.; Enright, G. D.; Wuest, J. D. *Angew. Chem., Int. Ed.* **2003**, *42*, 5303. (f) Wu, C.-D.; Hu, A.; Zhang, L.; Lin, W. *J. Am. Chem. Soc.* **2005**, *127*, 8940. (g) Tanabe, K. K.; Wang, Z.; Cohen, S. M. *J. Am. Chem. Soc.* **2008**, *130*, 8508. (h) Wang, Z.; Cohen, S. M. *Angew. Chem., Int. Ed.* **2008**, *47*, 4699. (i) Ahnfeldt, T.; Gunzelmann, D.; Loiseau, T.; Hirsemann, D.; Senker, J.; Férey, G.; Stock, N. *Inorg. Chem.* **2009**, *48*, 3057. (j) Ingleson, M. J.; Barrio, J. P.; Guilbaud, J.-B.; Khimyak, Y. Z.; Rosseinsky, M. J. *Chem. Commun.* **2008**, 2680. (k) Goto, Y.; Sato, H.; Shinkai, S.; Sada, K. *J. Am. Chem. Soc.* **2008**, *130*, 14354. (l) Morris, W.; Doonan, C. J.; Furukawa, H.; Banerjee, R.; Yaghi, O. M. *J. Am. Chem. Soc.* **2008**, *130*, 12626.

(3) (a) Grützmacher, H. *Angew. Chem., Int. Ed.* **2008**, *47*, 1814. (b) Gunanathan, C.; Ben-David, Y.; Milstein, D. *Science* **2007**, *317*, 790. (c) Weng, Z.; Teo, S.; Hor, T. S. A. *Acc. Chem. Res.* **2007**, *40*, 676.

(4) (a) Farha, O. K.; Shultz, A. M.; Sarjeant, A. A.; Nguyen, S. T.; Hupp, J. T. *J. Am. Chem. Soc.* **2011**, *133*, 5652. (b) Zhou, X.-P.; Xu, Z.; Zeller, M.; Hunter, A. D.; Chui, S. S.-Y.; Che, C.-M.; Lin, J. *Inorg. Chem.* **2010**, *49*, 7629. (c) Barron, P. M.; Wray, C. A.; Hu, C.; Guo, Z.; Choe, W. *Inorg. Chem.* **2010**, *49*, 10217. (d) Bloch, E. D.; Britt, D.; Lee, C.; Doonan, C. J.; Uribe-Romo, F. J.; Furukawa, H.; Long, J. R.; Yaghi, O. M. *J. Am. Chem. Soc.* **2010**, *132*, 14382. (e) Zhou, X.-P.; Xu, Z.; Zeller, M.; Hunter, A. D. *Chem. Commun.* **2009**, 5439. (f) Doonan, C. J.; Morris, W.; Furukawa, H.; Yaghi, O. M. *J. Am. Chem. Soc.* **2009**, *131*, 9492. (g) Dinca, M.; Long, J. R. *Angew. Chem., Int. Ed.* **2008**, *47*, 6766. (h) Wang, X.-S.; Ma, S.; Forster, P. M.; Yuan, D.; Eckert, J.; López, J. J.; Murphy, B. J.; Parise, J. B.; Zhou, H.-C. *Angew. Chem., Int. Ed.* **2008**, *47*, 7263. (i) Ma, S.; Sun, D.; Simmons, J. M.; Collier, C. D.;

Yuan, D.; Zhou, H.-C. *J. Am. Chem. Soc.* **2008**, *130*, 1012. (j) Ma, S.; Zhou, H.-C. *J. Am. Chem. Soc.* **2006**, *128*, 11734. (k) Seo, J. S.; Whang, D.; Lee, H.; Jun, S. I.; Oh, J.; Jeon, Y. J.; Kim, K. *Nature* **2000**, *404*, 982. (l) Chui, S. S. Y.; Lo, S. M. F.; Charmant, J. P. H; Orpen, A. G.; Williams, I. D. *Science* **1999**, *283*, 1148.

(5) (a) Vial, L.; Ludlow, R. F.; Leclaire, J.; Perez-Fernandez, R.; Otto, S. *J. Am. Chem. Soc.* **2006**, *128*, 10253. (b) He, J.; Yang, C.; Xu, Z.; Zeller, M.; Hunter, A. D.; Lin, J. *J. Solid State Chem.* **2009**, *182*, 1821. (c) He, J.; Yee, K.-K.; Xu, Z.; Zeller, M.; Hunter, A. D.; Chui, S. S.-Y.; Che, C.-M. *Chem. Mater.* **2011**, *23*, 2940.

(6) (a) Orgel, L. E. *J. Chem. Soc.* **1959**, 3815. (b) Walsh, A.; Payne, D. J.; Egdell, R. G.; Watson, G. W. *Chem. Soc. Rev.* **2011**, *40*, 4455.

(7) Rosi, N. L.; Kim, J.; Eddaoudi, M.; Chen, B.; O'Keeffe, M.; Yaghi, O. M. *J. Am. Chem. Soc.* **2005**, *127*, 1504.

(8) (a) Huang, G.; Tsang, C.-K.; Xu, Z.; Li, K.; Zeller, M.; Hunter, A. D.; Chui, S. S. Y.; Che, C.-M. *Cryst. Growth Des.* **2009**, *9*, 1444. (b) Huang, G.; Yang, C.; Xu, Z.; Wu, H.; Li, J.; Zeller, M.; Hunter, A. D.; Chui, S. S.-Y.; Che, C.-M. *Chem. Mater.* **2009**, *21*, 541.

(9) (a) Pearson, R. G. *J. Am. Chem. Soc.* **1963**, *85*, 3533. (b) Pearson, R. G. *Chemical Hardness*; Wiley-VCH: Weinheim, Germany, 1997.

(10) (a) Dai, Q.; Duty, C. E.; Hu, M. Z. *Small* **2010**, *6*, 1577. (b) Kamtekar, K. T.; Monkman, A. P.; Bryce, M. R. *Adv. Mater.* **2010**, *22*, 572. (c) Wu, H.; Ying, L.; Yang, W.; Cao, Y. *Chem. Soc. Rev.* **2009**, *38*, 3391. (d) Yang, Y.; Lowry, M.; Schowalter, C. M.; Fakayode, S. O.; Escobedo, J. O.; Xu, X.; Zhang, H.; Jensen, T. J.; Fronczek, F. R.; Warner, I. M.; Strongin, R. M. *J. Am. Chem. Soc.* **2006**, *128*, 14081. (e) Su, H.-C.; Chen, H.-F.; Fang, F.-C.; Liu, C.-C.; Wu, C.-C.; Wong, K.-T.; Liu, Y.-H.; Peng, S.-M. *J. Am. Chem. Soc.* **2008**, *130*, 3413. (f) Liu, J.; Cheng, Y.; Xie, Z.; Geng, Y.; Wang, L.; Jing, X.; Wang, F. *Adv. Mater.* **2008**, *20*, 1357. (g) Park, S.; Kwon, J. E.; Kim, S. H.; Seo, J.; Chung, K.; Park, S.-Y.; Jang, D.-J.; Medina, B. M.; Gierschner, J.; Park, S. Y. *J. Am. Chem. Soc.* **2009**, *131*, 14043. (h) Abbel, R.; Grenier, C.; Pouderoijen, M. J.; Stouwdam, J. W.; Leclère, P. E. L. G.; Sijbesma, R. P.; Meijer, E. W.; Schenning, A. P. H. J. *J. Am. Chem. Soc.* **2009**, *131*, 833. (i) Nandhikonda, P.; Heagy, M. D. *Chem. Commun.* **2010**, *46*, 8002. (j) Vijayakumar, C.; Sugiyasu, K.; Takeuchi, M. *Chem. Sci.* **2011**, *2*, 291. (k) Nandhikonda, P.; Heagy, M. D. *Org. Lett.* **2010**, *12*, 4796. (l) Hsu, C.-Y.; Liu, Y.-L. *J. Colloid Interface Sci.* **2010**, *350*, 75. (m) Zhang, C.; Huang, S.; Yang, D.; Kang, X.; Shang, M.; Peng, C.; Lin, J. *J. Mater. Chem.* **2010**, *20*, 6674. (n) Karpiuk, J.; Karolak, E.; Nowacki, J. *Phys. Chem. Chem. Phys.* **2010**, *12*, 8804. (o) Varghese, R.; Wagenknecht, H.-A. *Chem.—Eur. J.* **2009**, *15*, 9307.

(11) (a) Wang, M.-S.; Guo, G.-C.; Chen, W.-T.; Xu, G.; Zhou, W.-W.; Wu, K.-J.; Huang, J.-S. *Angew. Chem., Int. Ed.* **2007**, *46*, 3909. (b) Ki, W.; Li, J. *J. Am. Chem. Soc.* **2008**, *130*, 8114. (c) Liu, R.-S.; Drozd, V.; Bagkar, N.; Shen, C.-C.; Baginskiy, I.; Chen, C.-H.; Tan, C. H. *J. Electrochem. Soc.* **2008**, *155*, P71. (d) Law, G.-L.; Wong, K.-L.; Tam, H.-L.; Cheah, K.-W.; Wong, W.-T. *Inorg. Chem.* **2009**, *48*, 10492. (e) Wang, M.-S.; Guo, S.-P.; Li, Y.; Cai, L.-Z.; Zou, J.-P.; Xu, G.; Zhou, W.-W.; Zheng, F.-K.; Guo, G.-C. *J. Am. Chem. Soc.* **2009**, *131*, 13572. (f) Wei, Y.; Wu, K.; He, J.; Zheng, W.; Xiao, X. *CrystEngComm* **2011**, *13*, 52. (g) Wibowo, A. C.; Vaughn, S. A.; Smith, M. D.; zur Loye, H.-C. *Inorg. Chem.* **2010**, *49*, 11001.

(12) (a) Wibowo, A. C.; Smith, M. D.; zur Loye, H.-C. *Chem. Commun.* **2011**, *47*, 7371. (b) Wibowo, A. C.; Smith, M. D.; zur Loye, H.-C. *CrystEngComm* **2011**, *13*, 426. (c) Zhao, Y.-H.; Xu, H.-B.; Fu, Y.-M.; Shao, K.-Z.; Yang, S.-Y.; Su, Z.-M.; Hao, X.-R.; Zhu, D.-X.; Wang, E.-B. *Cryst. Growth Des.* **2008**, *8*, 3566. (d) Wang, X.-L.; Chen, Y.-Q.; Gao, Q.; Lin, H.-Y.; Liu, G.-C.; Zhang, J.-X.; Tian, A.-X. *Cryst. Growth Des.* **2010**, *10*, 2174. (e) Zhang, L.; Li, Z.-J.; Lin, Q.-P.; Qin, Y.-Y.; Zhang, J.; Yin, P.-X.; Cheng, J.-K.; Yao, Y.-G. *Inorg. Chem.* **2009**, *48*, 6517. (f) Yang, E. C.; Li, J.; Ding, B.; Liang, Q. Q.; Wang, X. G.; Zhao, X. J. *CrystEngComm* **2008**, *10*, 158. (g) Liu, Q.-Y.; Xu, L. *Eur. J. Inorg. Chem.* **2006**, *2006*, 1620. (h) Yang, J.; Li, G.-D.; Cao, J.-J.; Yue, Q.; Li, G.-H.; Chen, J.-S. *Chem.—Eur. J.* **2007**, *13*, 3248. (i) Nikol, H.; Vogler, A. *J. Am. Chem. Soc.* **1991**, *113*, 8988. (j) Dutta, S. K.; Perkovic, M. W. *Inorg. Chem.* **2002**, *41*, 6938. (k) Zhao, Y.-H.; Xu, H.-B.; Shao, K.-Z.; Xing, Y.; Su, Z.-M.; Ma, J.-F. *Cryst. Growth Des.* **2007**, *7*, 513. (l) Zhu, X.; Li, X.; Liu, Q.; Lü, J.; Guo, Z.; He, J.; Li, Y.; Cao, R. *J. Solid State Chem.* **2007**, *180*, 2386. (m) Strasser, A.; Vogler, A. *Inorg. Chem. Commun.* **2004**, *7*, 528.

(13) Feng, P. L.; Perry, J. J. I. V.; Nikodemski, S.; Jacobs, B. W.; Meek, S. T.; Allendorf, M. D. *J. Am. Chem. Soc.* **2010**, *132*, 15487.

(14) (a) Porrès, L.; Holland, A.; Pålsson, L.-O.; Monkman, A. P.; Kemp, C.; Beeby, A. *J. Fluoresc.* **2006**, *16*, 267. (b) Pålsson, L.-O.; Monkman, A. P. *Adv. Mater.* **2002**, *14*, 757. (c) De Mello, J. C.; Wittmann, F. H.; Friend, R. H. *Adv. Mater.* **1997**, *9*, 230.

(15) Murase, N.; Li, C. *J. Lumin.* **2008**, *128*, 1896.

(16) Bowers, M. J. II; McBride, J. R.; Rosenthal, S. J. *J. Am. Chem. Soc.* **2005**, *127*, 15378.

(17) see http://en.wikipedia.org/wiki/CIE_1931_color_space for more details.

(18) (a) Ok, K. M.; Chi, E. O.; Halasyamani, P. S. *Chem. Soc. Rev.* **2006**, *35*, 710. (b) Maury, O.; Le Bozec, H. *Acc. Chem. Res.* **2005**, *38*, 691. (c) Evans, O. R.; Lin, W. *Acc. Chem. Res.* **2002**, *35*, 511. (d) Zyss, J. *Molecular Nonlinear Optics: Materials, Physics, and Devices*; Academic Press: New York, 1993. (e) Agulló-López, F.; Cabrera, J. M.; Agulló-Rueda, F. *Electroptics: Phenomena, Materials and Applications*; Academic Press: New York, 1994. (f) Lin, W.; Evans, O. R.; Xiong, R.-G.; Wang, Z. *J. Am. Chem. Soc.* **1998**, *120*, 13272. (g) Swift, J. A.; Ward, M. D. *Chem. Mater.* **2000**, *12*, 1501. (h) Ye, Q.; Song, Y.-M.; Wang, G.-X.; Chen, K.; Fu, D.-W.; Chan, P. W. H.; Zhu, J.-S.; Huang, S. D.; Xiong, R.-G. *J. Am. Chem. Soc.* **2006**, *128*, 6554. (i) Zhang, W.; Xiong, R.-G.; Huang, S. D. *J. Am. Chem. Soc.* **2008**, *130*, 10468. (j) Wang, G.-X.; Han, G.-F.; Ye, Q.; Xiong, R.-G.; Akutagawa, T.; Nakamura, T.; Chan, P. W. H.; Huang, S. D. *Dalton Trans.* **2008**, 2527. (k) Zhao, H.; Ye, Q.; Qu, Z.-r.; Fu, D.-W.; Xiong, R.-G.; Huang, S. D.; Chan, P. W. H. *Chem.—Eur. J.* **2008**, *14*, 1164.

(19) (a) Holman, K. T.; Pivovar, A. M.; Ward, M. D. *Science* **2001**, *294*, 1907. (b) Holman, K. T.; Pivovar, A. M.; Swift, J. A.; Ward, M. D. *Acc. Chem. Res.* **2001**, *34*, 107.

(20) (a) Li, K.; Xu, Z.; Xu, H.; Carroll, P. J.; Fettinger, J. C. *Inorg. Chem.* **2006**, *45*, 1032. (b) Huang, G.; Xu, H.; Zhou, X.-P.; Xu, Z.; Li, K.; Zeller, M.; Hunter, A. D. *Cryst. Growth Des.* **2007**, *7*, 2542.

(21) (a) Lin, W.; Wang, Z.; Ma, L. *J. Am. Chem. Soc.* **1999**, *121*, 11249. (b) Liu, Y.; Xu, X.; Zheng, F.; Cui, Y. *Angew. Chem., Int. Ed.* **2008**, *47*, 4538.

(22) Sun, Y.-Q.; He, J.; Xu, Z.; Huang, G.; Zhou, X.-P.; Zeller, M.; Hunter, A. D. *Chem. Commun.* **2007**, 4779.

(23) Kurtz, S. K.; Perry, T. T. *J. Appl. Phys.* **1968**, *39*, 3798.